

Sensitivity of Shear Strength of Reinforced Concrete and Prestressed Concrete Beams to Shear Friction and Concrete Softening According to Modified Compression Field Theory

by Dat Duthinh

The modified compression field theory (MCFT) is used to study the effect of shear friction and biaxial softening on the computed shear strength of reinforced (RC) or prestressed concrete (PC) beams. A comparison is presented of the various relationships that have been proposed to represent the shear friction behavior of cracked reinforced concrete. A decrease in shear friction within the range of experimental data as found, for example, in high-strength concrete, can lower the shear strength of beams with minimum shear reinforcement by 15 to 25 percent, according to the MCFT.

In addition, a comparison is presented of different relationships used to represent the biaxial compression-tension strength of reinforced concrete for RC and PC beams. Some theories of biaxial softening of concrete do not predict concrete crushing even for very high deformations, but rather show significant shear force gain after stirrup yielding and crack slipping. For the RC beam example, some theories predict shear tension failure while others predict diagonal compression failure. However, the first peaks of shear load, which occur close to stirrup yielding and crack slipping, are within 10 percent of one another for the various theories and within 10 percent of the test value for the PC beam.

Keywords: aggregate interlock; beams; compression; prestressed concrete; reinforced concrete; shear.

INTRODUCTION

The importance of aggregate interlock, or shear-friction, across shear cracks, as one of the mechanisms of shear resistance in reinforced concrete (RC) beams has been recognized for quite some time. (Fig. 1 adapted from MacGregor, 1992; and from Joint ASCE-ACI Task Committee 426, 1990.) However, traditional ACI beam design equations for shear (ACI 318-95) do not take explicit account of shear friction, but rather lump it together with other factors, such as dowel effect and the shear carrying capacity of the compressed part of the beam into the concrete contribution term V_c .

In the last 20 years, more rational methods for shear strength calculation have been able to explicitly account for the contribution of shear friction across cracks in resisting shear. One noteworthy method that has now been adopted in the Canadian Code (CSA A 23.3-94), the Norwegian Code (NS 3473 E 1992), and the AASHTO LRFD Bridge Design Specifications (1994) is the modified compression field theory (MCFT) (Vecchio and Collins, 1986; Collins and Mitchell, 1991).

Another aspect of shear cracks is that they also weaken the concrete struts. The presence of transverse tensile stress and strain lowers the concrete compressive strength below its uniaxial strength (softening). The MCFT provides a means to evaluate the effect of this softening on the shear strength of RC beams.

Following reviews of the MCFT and other works on shear friction and biaxial softening, this paper presents the results of a

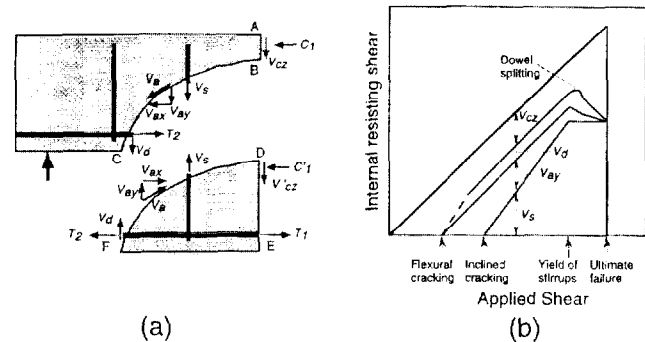


Fig. 1—(a) Internal forces in cracked beam with stirrups; and (b) relative magnitude of shear carrying mechanisms: V_s , due to stirrups; V_{ay} due to aggregate interlock; V_d due to dowel action; and V_{cz} due to compression zone of beam (adapted from MacGregor, 1992).

parametric study that determines the effects of changes in shear friction and concrete softening on the shear strength of RC and prestressed concrete (PC) beams, as predicted by the MCFT.

RESEARCH SIGNIFICANCE

The shear strength of RC and PC beams remains an active area of research, especially with the advent of high-strength concretes (HSC) that are beginning to exceed the database (largely below 40 MPa) of the ACI design equations. Current ACI Code shear design equations limit f'_c to 69 MPa, although higher strength concrete is allowed provided that the minimum shear reinforcement is increased accordingly. In the last 20 years, rational methods have been developed that incorporate the knowledge of the friction laws of shear cracks and the softening of concrete under biaxial compression and tension. This paper studies the sensitivity of the shear strength of RC and PC beams, computed according to the MCFT, to softening models and changes in shear friction, with a view of clarifying future research directions aimed at codifying the use of high-strength concrete in structures.

REVIEW OF MODIFIED COMPRESSION FIELD THEORY (MCFT)

The MCFT is a rational theory capable of predicting the strength of reinforced and prestressed concrete beams under

ACI Structural Journal, V. 96, No. 4, July-August 1999.
Received August 7, 1997, and reviewed under Institute publication policies. Copyright © 1999, American Concrete Institute. All rights reserved, including the making of copies unless permission is obtained from the copyright proprietors. Pertinent discussion will be published in the May-June 2000 ACI Structural Journal if received by January 1, 2000.

ACI member Dat Duthinh is a research structural engineer with the Building and Fire Research Laboratory of the National Institute of Standards and Technology in Gaithersburg, Md. He is a member of ACI Committees 363, High-Strength Concrete; 440, Fiber Reinforced Polymer Reinforcement; and Joint ACI-ASCE Committee 445, Shear and Torsion. His research interests include high-strength concrete, shear strength, and use of fiber reinforced polymers for structural members and repairs.

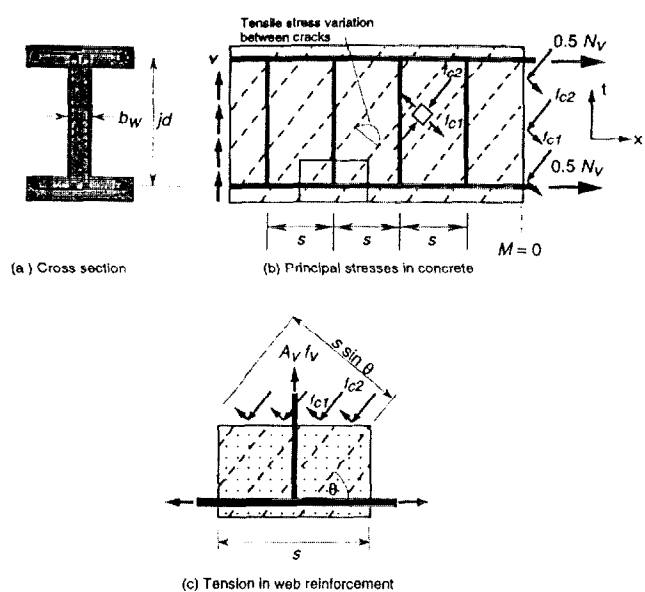


Fig. 2—Equilibrium conditions for modified compression field theory (Collins and Mitchell, 1991).

shear and axial loading. It is rational in the sense that it satisfies equilibrium of forces and moments, compatibility of displacements, and the stress-strain relationships of concrete and reinforcing steel. One of the simplifying assumptions of the MCFT is that the principal directions of stress and strain coincide. According to the MCFT, the shear strength V of a RC beam is the sum of a steel contribution V_s and a concrete contribution V_c . The steel contribution is based on the variable angle θ truss model, whereas the concrete contribution is the shear resisted by tensile stresses f_{c1} in the diagonally cracked concrete (Fig. 2). The concrete tensile stress f_{c1} is zero at cracks, and reaches a maximum halfway between cracks. (The notation is explained in Fig. 2 and at the end of the paper).

$$V = V_s + V_c = \frac{A_v f_v}{s} j d \cot \theta + f_{c1} b_w j d \cot \theta \quad (1)$$

The concrete contribution, which depends on f_{c1} , is a function of the shear that can be transmitted across cracks by aggregate interlock. Indeed, after yielding of the transverse reinforcement, transmittal of tension across cracks requires local shear stresses τ along cracks. The ability of the crack interface to transmit the shear stress τ depends strongly on the crack width w . Vecchio and Collins (1986) allowed for the possibility of local compressive normal stress σ across cracks. Based on Walraven and Reinhardt's (1981) experimental results, they suggested the following parabolic relation of τ to σ (Fig. 3 from Vecchio and Collins, 1986)

$$\frac{\tau}{\tau_{max}} = 0.18 + 1.64 \frac{\sigma}{\tau_{max}} - 0.82 \left(\frac{\sigma}{\tau_{max}} \right)^2 \quad (2a)$$

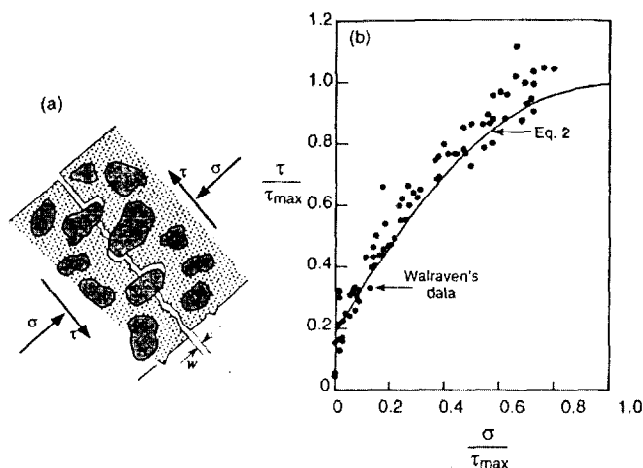


Fig. 3—(a) Transmission of shear stress across crack by aggregate interlock; and (b) relationship between shear stress transmitted across crack and compressive stress on crack (adapted from Vecchio and Collins, 1986).

$$\text{with } \tau_{max}/\text{MPa} = \frac{\sqrt{f'_c}/\text{MPa}}{0.3 + \frac{24w}{c + 16\text{mm}}} \quad (2b)$$

Thus, τ_{max} , the maximum shear stress transmissible across a crack is a function of the crack width w , the concrete strength f'_c and the maximum aggregate size c . As the normal stress σ across cracks increases, so does the shear stress τ , but not quite as steeply as a linear relationship with a cohesion term. It turns out that, in most practical situations, σ has a negligible effect, hence, Eq. (2a) was simplified in later versions of the MCFT to (Collins and Mitchell, 1991)

$$\tau = 0.18 \tau_{max} \quad (3)$$

The MCFT assumes a parabolic relationship (Hognestad, 1952) to describe the stress-strain behavior of concrete in compression

$$\frac{f_{c2}}{f_{c2max}} = 2 \left(\frac{\epsilon_2}{\epsilon_0} \right) - \left(\frac{\epsilon_2}{\epsilon_0} \right)^2 \quad (4)$$

where ϵ_0 is the strain at peak uniaxial stress, and f_{c2max} which is the compressive strength of concrete panels in biaxial tension (Direction 1) – compression (Direction 2), depends on the transverse tensile strain ϵ_1 . A softening parameter β is defined as the ratio of f_{c2max} to the uniaxial cylinder compressive strength f'_c [Fig. 8(b)].

$$\beta = \frac{f_{c2max}}{f'_c} = \frac{1}{0.80 + 0.34 \epsilon_1 / \epsilon_0} \leq 1.0 \quad (5)$$

Eq. (5) was derived from panel tests with a mean ratio of test values to equation predictions of 0.98 and a coefficient of variation for the same ratio of 0.16

$$\text{For } \epsilon_0 = 0.002, \beta = \frac{1}{0.80 + 170 \epsilon_1} \quad (6)$$

Eq. (6) is used in the Canadian Code (CSA, 1994). Thus, the principal compressive stress in the concrete f_{c2} is a function not

only of the principal compressive strain ϵ_2 , but also of the co-existing principal tensile strain ϵ_1 .

REVIEW OF SHEAR FRICTION

Walraven and Reinhardt (1981), and Walraven (1981) performed some important work on the constitutive relations of shear cracks in concrete. Their work accounts for aggregate interlock, dowel action, and axial tension of the reinforcement crossing a shear crack, combines experiment and theory, and shows good agreement between the two.

Direct shear tests with no bending were conducted on pre-cracked, pushoff, rectangular specimens 400 x 600 x 120 mm with a shear area of 300 x 120 mm. The two applied loads were collinear with the crack, and wedges on the upper and lower faces of the specimen channeled the loads to either side of the crack (Fig. 4). The specimens were either internally or externally reinforced, with the cube strength f_{cc} of concrete ranging from 20 to 56 MPa, and included a lightweight concrete and one mix with a discontinuous grading of aggregate size (no aggregate between 0.25 and 1.00 mm. The other mixes had a distribution of aggregate sizes). The reinforcement ranged in ratio from 0.56 to 3.35 percent, and in inclination from 45 to 135 deg to the crack plane. In one series of experiments, the reinforcement bars were covered with soft sleeves extending 20 mm on both sides of the crack to eliminate dowel action. During the tests, crack displacements were recorded versus the applied shear force. In addition, for the externally reinforced specimens, the normal restraint force exerted by the reinforcement crossing the plane of the crack was measured. Thus, curves of shear stress and normal stress versus crack slip for various values of crack width could be plotted for the externally reinforced specimens (Fig. 5). Walraven and Reinhardt (1981) noticed that the behavior of the internally reinforced specimens was totally dif-

ferent from that of the externally reinforced ones. The crack displacement path (curve of crack width versus crack slip) was much more sensitive to the stiffness of the reinforcement for the externally reinforced specimens than for the internally reinforced ones. Nevertheless, Walraven and Reinhardt used the same model of aggregate interlock for both types of specimens. In addition to aggregate interlock, the shear crack model of the internally reinforced specimens also included the dowel action of the reinforcement and its bond to concrete.

The analytical model of aggregate interlock assumes the concrete to be composed of two phases: a rigid, perfectly plastic mortar, and rigid, spherical aggregates of various sizes [Fig. 5(a) and

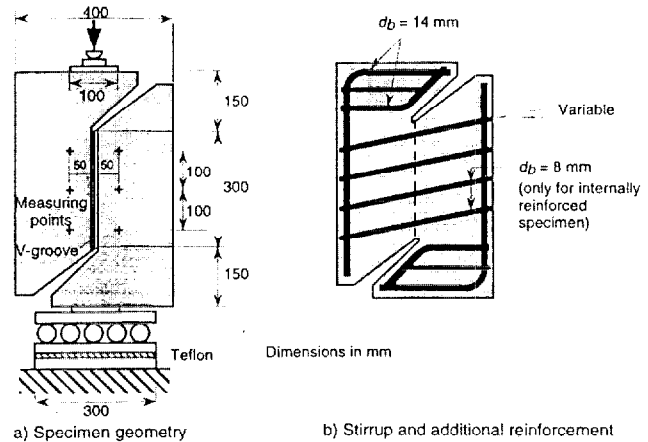


Fig. 4—Pushoff test specimens to study aggregate interlock in cracked reinforced concrete: (a) geometry; and (b) reinforcement (Walraven and Reinhardt, 1981).

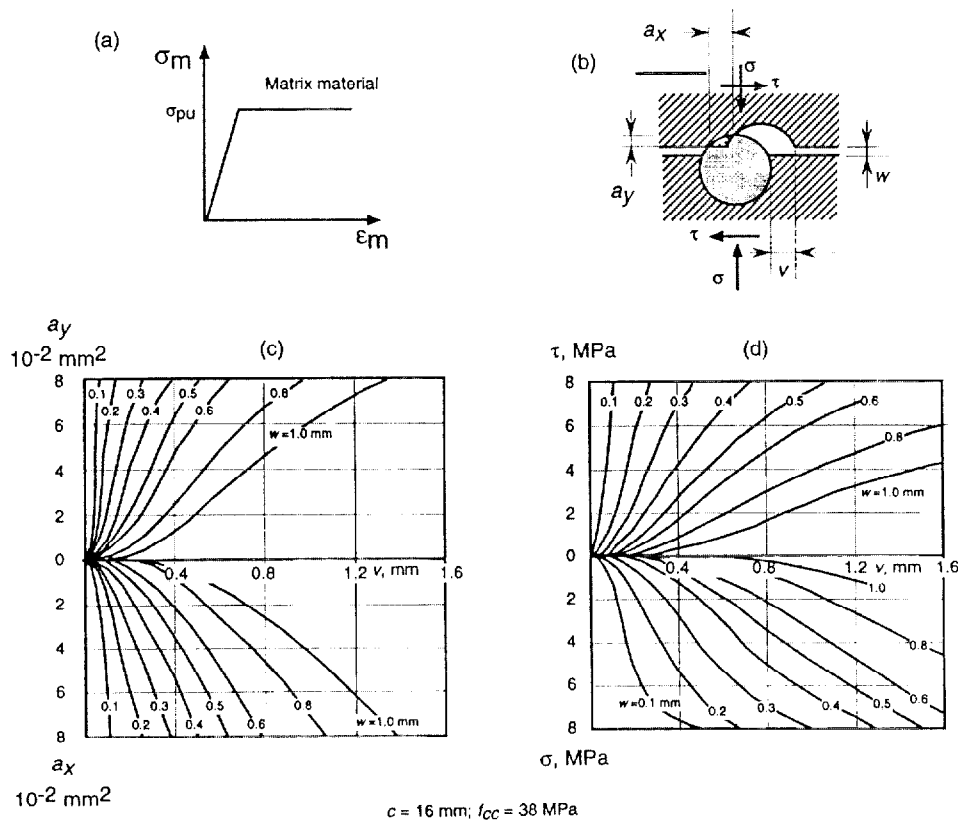


Fig. 5—Walraven's model for shear transfer across crack: (a) stress-strain curve of matrix material; (b) deformation at crack; (c) contact areas as functions of crack width and slip; and (d) normal and shear stresses as functions of crack width and slip (adapted from Fréney, 1990).

(b)]. Knowing the volumetric ratio of aggregate to concrete and the size distribution of the aggregate, one can work out the average number of aggregate particles encountered by a crack of a given length. The portion of the mortar that interferes geometrically with the aggregate when the crack faces open and slide with respect to one another is assumed to yield, thus engendering normal and shear stresses that are related by a coefficient of friction μ . Equilibrium is related to frictional sliding and crushing of matrix material along the projected contact areas a_x and a_y . These depend on the crack slip v , opening w , and the mix proportions (maximum aggregate size and volumetric percentage of aggregate). The constitutive equations for the analytical model of the cracked specimens are

$$\sigma = \sigma_{pu}(A_x - \mu A_y) \quad \text{and} \quad \tau = \sigma_{pu}(A_y + \mu A_x) \quad (7)$$

where A_x and A_y , the nondimensionalized sums of a_x and a_y , depend on the crack width w , the crack slip v , the maximum particle diameter c , and the total aggregate volume per unit volume of concrete [Fig. 5(b) and (c)]. The strength of the mortar σ_{pu} , assumed to be elastic-perfectly plastic [Fig. 5(a)], and the coefficient of friction μ between mortar and aggregate were found from fitting curves to the experimental results

$$\mu = 0.40 \quad \text{and} \quad \sigma_{pu}/\text{MPa} = 6.39(f_{cc}/\text{MPa})^{0.56} \quad (8)$$

Physically reasonable values can be found that fit all experimental curves well, thus lending credibility to the theory. [The indeterminacy of the two parameters μ and σ_{pu} in Eq. (7) means that two curves, such as those shown in Fig. 5(d), can always be fitted well. The credibility of the theory lies in the good fit of all the curves.]

After performing further tests of 88 pushoff internally-reinforced specimens with compressive strengths ranging from 17 to 60 MPa, Walraven, Fréney, and Puijssers (1987) developed the following empirical expression for the shear friction capacity of internally reinforced cracks as a function of concrete strength and amount of reinforcement, but not of aggregate size

$$\tau_{max}/\text{MPa} = C_1(\rho_v f_y/\text{MPa}) \quad (9)$$

in which $C_1 = 0.822(f_{cc}/\text{MPa})^{0.406}$ and $C_2 = 0.159(f_{cc}/\text{MPa})^{0.303}$

f_{cc} is the concrete compressive strength of 150-mm cubes, and ρ_v and f_y are the cross-sectional area ratio and yield strength of the shear reinforcement, respectively. Comparison between theoretical values of τ_{max} according to Eq. (9) and experimental results by Hofbeck, Ibrahim, and Mattock (1969), Walraven and Reinhardt (1981), Fréney (1985), and Puijssers and Liqui Lung (1985) produced excellent agreement (mean = 1.001, standard deviation = 0.109 for the ratio experimental/theoretical values).

Mau and Hsu's formula (1988) works well for the shear capacity of cracks in normal strength reinforced concrete

$$\frac{\tau_{max}}{f'_c} = 0.66\sqrt{\omega} < 0.3 \quad \text{with} \quad \omega = \frac{\rho_v f_y}{f'_c} \quad (10)$$

When applied to the same test results, Eq. (10) performed almost as well as Eq. (9), and is much simpler to use (mean = 1.019, standard deviation = 0.127 for the ratio experimental/theoretical values). Again, aggregate size is not a factor.

Since crack surfaces are smoother in HSC than in normal strength concrete (NSC)—cracks tend to go through the aggregate in HSC, whereas they go around the aggregate in NSC—one would expect a decrease in shear friction as the concrete strength increases. This is indeed the case, as was

born out by shear friction tests on precracked pushoff specimens made of concrete with a cylinder strength of 100 MPa, or a cube strength of 115 MPa (Fréney et al., 1987; Walraven and Stroband, 1994; and Walraven, 1995). Shear-friction at a given crack slip and opening for HSC (for example, 100 MPa) is reduced to 35 percent of its value for NSC (with compressive strength between, for example, 40 and 60 MPa) for externally reinforced specimens, and between 55 to 75 percent for internally reinforced ones. The constitutive equations of the model for cracks in HSC are then

$$\sigma = k\sigma_{pu}(A_x - \mu A_y) \quad \text{and} \quad \tau = k\sigma_{pu}(A_y + \mu A_x) \quad (11)$$

with $k = 0.35$ for externally reinforced HSC, and $k = 0.65$ for internally reinforced HSC.

Besides the MCFT, other theories of beam shear strength also use Walraven's experimental results to account for shear friction. Reineck (1982, 1991) used the following constitutive equations for the friction of crack faces

$$\tau = \tau_{f0} + 1.7\sigma = \tau_{f0} \frac{v - 0.24w}{0.096w + 0.01 \text{ mm}} \quad (12)$$

The cohesion friction stress τ_{f0} is the limiting value of shear strength without normal stress σ on the crack face

$$\tau_{f0} = 0.45f_i \left(1 - \frac{w}{0.9 \text{ mm}}\right) \quad (13)$$

where f_i is the concrete tensile strength.

Kupfer and Bulicek (1991) used the following relationships from Walraven and Reinhardt (1981)

$$\frac{\tau}{\text{MPa}} = -\frac{f_{cc}}{30 \text{ MPa}} + \left(1.8 \left(\frac{w}{\text{mm}}\right)^{-0.8} + \right. \quad (14)$$

$$\left. \left(0.234 \left(\frac{w}{\text{mm}}\right)^{-0.707} - 0.20 \right) \frac{f_{cc}}{\text{MPa}} \right) \frac{v}{\text{mm}} \geq 0$$

$$\frac{\sigma}{\text{MPa}} = \frac{f_{cc}}{20 \text{ MPa}} - \left(1.35 \left(\frac{w}{\text{mm}}\right)^{-0.63} + \right.$$

$$\left. 0.191 \left(\frac{w}{\text{mm}}\right)^{-0.552} - 0.15 \right) \frac{f_{cc}}{\text{MPa}} \frac{v}{\text{mm}} \leq 0$$

Earlier, Kupfer, Mang and Karavesyrogrou (1983) used

$$\frac{\tau}{f'_c} = 0.117 - 0.085 \frac{v}{\text{mm}} \quad \text{for Case A: } v = w \quad (15a)$$

$$\frac{\tau}{f'_c} = 0.017 + 0.1 \frac{v}{w} - 0.085 \frac{v}{\text{mm}} \quad \text{for Case B: } v \neq w \quad (15b)$$

These equations were based on earlier work by Walraven and derived from experiments performed on concrete with compressive strength of 25 MPa and for $v > 0.20$ mm. In beams, Case A arises when the average strain of both flanges equals the longitudinal component of the normal strain of the

compression struts. This situation occurs in prestressed beams. In Case B, the average strain of both chords is zero.

Dei Poli, Prisco, and Gambarova (1990) used a rough crack model (Bazant and Gambarova, 1980) to describe aggregate interlock in their theory of beam shear strength

$$\sigma = 0.62 \frac{r\sqrt{w/\text{mm}}\tau}{(1+r^2)^{0.25}} \quad (16)$$

$$\tau = 0.25f'_c \left(1 - \sqrt{\frac{2w}{c}}\right) r \frac{a_3 + a_4|r|^3}{1 + a_4r^4}$$

where

$$\begin{aligned} a_3 &= 9.8 \text{ MPa}/f'_c; \\ a_4 &= 2.44 - 39 \text{ MPa}/f'_c; \text{ and} \\ r &= v/w. \end{aligned}$$

In earlier work based on tests by Paulay and Loeber (1974), Bazant and Gambarova (1980) suggested the following formulas, which were later updated to Eq. (16) for shear stress τ and normal compressive stress σ in cracks of concrete members as functions of crack opening w and slip v :

$$\frac{\sigma}{\text{MPa}} = \frac{0.534 \text{ mm}}{1000w} \left(145 \left| \frac{\tau}{\text{MPa}} \right| \right)^p \quad (17)$$

$$\text{and } \tau = \tau_{\max} r \frac{a_3 + a_4|r|^3}{1 + a_4r^4}$$

$$\text{with } \tau_{\max} = 0.245f'_c \frac{c^2}{c^2 + 100w^2} \text{ and}$$

$$p = 1.30 \left(1 - \frac{0.231}{1 + 0.185(w/\text{mm}) + 5.63(w/\text{mm})^2}\right)$$

where

$$\begin{aligned} a_3 &= 10 \text{ MPa}/f'_c; \\ a_4 &= 2.44 - 39.8 \text{ MPa}/f'_c; \text{ and} \\ r &= v/w. \end{aligned}$$

A comparison of various relationships for shear and normal stresses versus crack slip for two crack openings ($w = 0.5$ or 0.8 mm) is shown in Fig. 6. The curves are based on $f_{\alpha} = 59$ MPa, $f'_c = 50.2$ MPa, $f_t = 3.5$ MPa, and $c = 16$ mm. Also shown are experimental data from Walraven and Reinhardt (1981). The following can be observed.

- Walraven and Reinhardt's (1981) Eq. (14) is a good approximation of their experimental data in the linear range. However, the equations need to have a cap so shear and normal stresses do not increase indefinitely as crack slip increases.
- Reineck's (1991) Eq. (12) and (13) also need to have a cap. They approximate the experimental data well for a crack width of $w = 0.5$ mm, but not for $w = 0.8$ mm.
- Dei Poli, Prisco, and Gambarova's (1990) Eq. (16) and Bazant and Gambarova's (1980) Eq. (17) follow the general trend of the data, but there are significant deviations from Walraven's experimental data. A fine tuning of the parameters of the models could bring better agreement.
- Kupfer, Mang, and Karavesyoglou's (1983) Eq. (15b) is based on weaker concrete and does not agree well with Walraven and Reinhardt's (1981) experimental data.

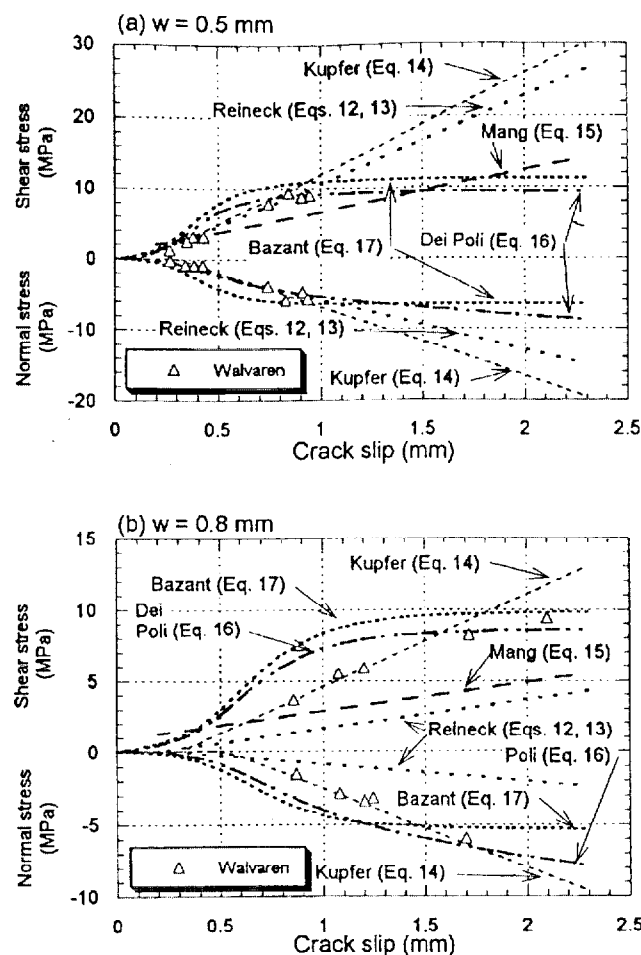


Fig. 6—Crack behavior according to various researchers.

REVIEW OF CONCRETE SOFTENING

The web of reinforced concrete beams under shear is in a state of biaxial tension-compression. The presence of simultaneous transverse tensile strain leads to a deterioration of the compressive strength of cracked concrete (Fig. 7). This softening behavior has been investigated in panel tests.

Vecchio and Collins (1993) reviewed various models of compression softening of cracked reinforced concrete panels due to transverse tension. The following is adapted from their review. In an early study, Vecchio and Collins (1982) expressed β as a function of the ratio of the principal strains

$$\beta = \frac{1}{0.85 - 0.27\epsilon_1/\epsilon_2} \quad (18)$$

where ϵ_1 is the principal tensile strain, averaged over several cracks. Vecchio and Collins used Hognestad's (1952) parabola for the uniaxial compressive stress-strain curve of concrete. Both peak stress f'_c and its associated strain ϵ_0 were multiplied by β [Fig. 8(a)]. Good agreement was found with 178 experimental data points (mean ratio = 1.01, coefficient of variation = 0.15).

Kollegger and Mehlhorn (1987, 1990) concluded that the effective compressive strength did not reduce beyond $0.8f'_c$ and that the prime influencing factor appeared to be the principal tensile stress f_{c1} rather than the principal tensile strain ϵ_1 . The value of β was given for different values of normalized tensile stress as follows

$$\text{for } 0 \leq f_{c1}/f_t \leq 0.25, \beta = 1.0 \quad (19)$$

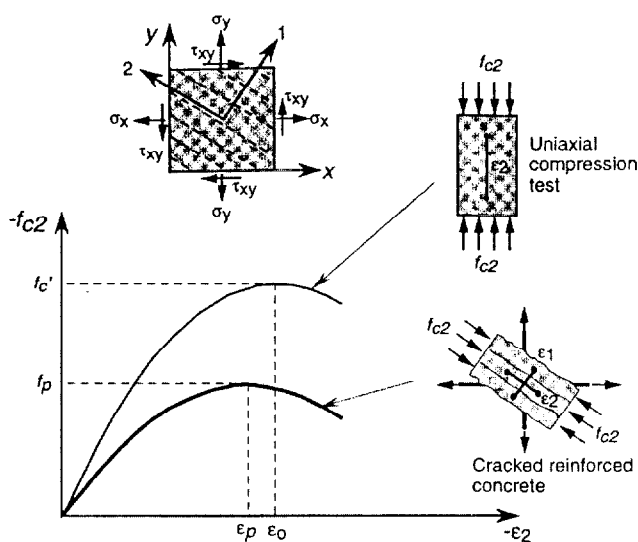


Fig. 7—Deteriorated compression response in cracked reinforced concrete elements (Vecchio and Collins, 1993).

$$\text{for } 0.25 < f_{c1}/f_t < 0.75, \beta = 1.1 - 0.4f_{c1}/f_t$$

$$\text{and for } 0.75 \leq f_{c1}/f_t \leq 1.0, \beta = 0.8$$

They based their conclusions on 55 panel tests that had the tension-compression loads applied parallel to the reinforcement in most tests, but with some applied at 45 deg.

Miyahara et al.(1988) proposed a softening model based on the principal tensile strain

$$\text{for } \epsilon_1 \leq 0.0012, \beta = 1.0 \quad (20)$$

$$\text{for } 0.0012 < \epsilon_1 < 0.0044, \beta = 1.15 - 125\epsilon_1$$

$$\text{and for } 0.0044 \leq \epsilon_1, \beta = 0.60$$

The degree of softening is much less than that predicted by Vecchio and Collins.

Shirai and Noguchi (1989) and Mikame et al. (1991) proposed the following relationship for the softening parameter

$$\beta = \frac{1}{0.27 + 0.96(\epsilon_1/\epsilon_0)^{0.167}} \quad (21)$$

They noted that the softening is greater for HSC than for NSC.

For HSC, Ueda et al.(1991) proposed the following

$$\beta = \frac{1}{0.8 + 0.6(1000\epsilon_1 + 0.2)^{0.39}} \quad (22)$$

Vecchio and Collins (1993) updated their model as follows. Their new base uniaxial stress-strain curve is the Thorenfeldt (1987) curve [Fig. 8(c)], which is more appropriate for HSC (more linear in its pre-ultimate response) than Hognestad's parabola [Fig. 8(a)]. The parameters for the Thorenfeldt curve were determined by Collins and Porasz (1989)

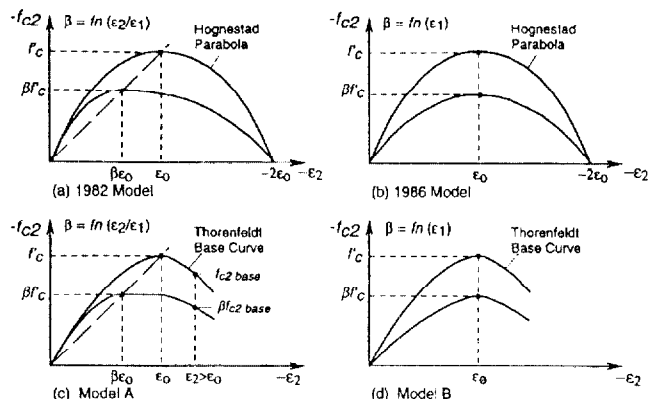


Fig. 8—Compression softening models: (a) 1982 model; (b) 1986 models; (c) proposed Model A; and (d) proposed Model B (Vecchio and Collins, 1993).

$$f_{c2base} = -f_p \frac{n(-\epsilon_2/\epsilon_p)}{n-1 + (-\epsilon_2/\epsilon_p)^k} \quad (23)$$

where

$$n = 0.80 + f_p/(17 \text{ MPa}); \quad (24)$$

$$k = 1.0 \text{ for } -\epsilon_p < \epsilon_2 < 0;$$

$$k = 0.67 + f_p/(62 \text{ MPa}) \text{ for } \epsilon_2 < -\epsilon_p;$$

f_p = maximum compressive stress for softened concrete.

Eq. (23) and (24) are used with $f_p = \beta f'_c$ and $\epsilon_p = \epsilon_0$ = strain in uniaxial compression at peak stress f'_c . The base stress-strain curve is modified in two possible ways.

Model A uses strength and strain softening, i.e., both peak stress and its corresponding strain decrease [Fig. 8(c)]

$$\beta = \frac{1}{1.0 + K_c K_f} \quad (25)$$

where

$$K_c = 0.35 \left(\frac{-\epsilon_1}{\epsilon_2} - 0.28 \right)^{0.80} \geq 1.0 \text{ for } \epsilon_1 < \epsilon_{1L},$$

$$\text{and } K_f = 0.1825 \sqrt{f'_c / \text{MPa}} \geq 1.0.$$

ϵ_{1L} is the limiting tensile strain in the concrete at which the reinforcement at a crack begins to yield and the concrete suffers little additional cracking. The curve is divided into three parts:

Prepeak—for $-\epsilon_2 < \beta\epsilon_0, f_{c2}$ is calculated from Eq. (23) with $f_p = \beta f'_c$ and $\epsilon_p = \beta\epsilon_0$;

Peak—for $\beta\epsilon_0 \leq -\epsilon_2 \leq \epsilon_0, f_{c2} = f_p = \beta f'_c$; and

Postpeak—for $-\epsilon_2 > \epsilon_0, f_{c2} = \beta f_{c2base}$ with f_{c2base} calculated from Eq. (23) using $f_p = f'_c$ and $\epsilon_p = \epsilon_0$.

Note that $K_f \geq 1$ for $f'_c \geq 30 \text{ MPa}$ and $K_c \geq 1$ for $-\epsilon_1 / \epsilon_2 \geq 4$.

Model B uses strength-only softening [Fig. 8(d)]

$$\beta = \frac{1}{1 + K_c} \text{ where } K_c = 0.27 \left(\frac{\epsilon_1}{\epsilon_0} - 0.37 \right) \quad (26)$$

In a later update, Vecchio, Collins, and Aspiotis (1994) conducted 12 shear tests of panels 890 x 890 x 70 mm made of 55-MPa concrete. The panels were reinforced by two orthogonal grids at 45 deg to their edges. Results show that the compression-softening formulation developed for NSC elements applies equally well to HSC elements. Now Model B also has a K_f factor

$$K_f = 2.55 - 0.2629 \sqrt{f'_c / \text{MPa}} \leq 1.11 \quad (27)$$

Both models agree well with experiments, with the updated Model B being slightly superior.

Belarbi and Hsu (1991) also used Hognestad's parabola as a basis and suggested one softening parameter for stress and another for strain

$$\beta_\sigma = \frac{0.9}{\sqrt{1 + K_\sigma \epsilon_1}} \text{ and } \beta_\epsilon = \frac{1}{\sqrt{1 + K_\epsilon \epsilon_1}} \quad (28)$$

where K_σ and K_ϵ depend on the orientation ϕ of the cracks to the reinforcement and the type of loading in the biaxial test as follows

ϕ	Proportional loading		Sequential loading	
	K_σ	K_ϵ	K_σ	K_ϵ
45 deg	400	160	400	160
90 deg	400	550	250	0

In a later paper, Belarbi and Hsu (1995) presented the results of tests of 22 panels of 1400 x 1400 x 178 mm under biaxial tension-compression. The panels had a concrete strength of 40 MPa, minimal reinforcement (0.54 percent) in the compression (transverse) direction, and various reinforcement ratios in the tension (longitudinal) direction. For a nonsoftened standard cylinder, stress is a parabolic function of strain as in Hognestad's equation. The following stress-strain relationship is proposed for softening [Fig. 8(a)]

$$\text{For } \epsilon_2 \leq \beta \epsilon_0 \quad f_{c2} = \beta f'_c \left[2 \left(\frac{\epsilon_2}{\beta \epsilon_0} \right) - \left(\frac{\epsilon_2}{\beta \epsilon_0} \right)^2 \right] \quad (29)$$

$$\text{For } \epsilon_2 > \beta \epsilon_0 \quad f_{c2} = \beta f'_c \left[1 - \left(\frac{\frac{\epsilon_2}{\beta \epsilon_0} - 1}{\frac{2}{\beta} - 1} \right)^2 \right]$$

$$\beta = \frac{0.9}{\sqrt{1 + K_\sigma \epsilon_1}}$$

where

$K_\sigma = 400$ for proportional loading; or

$K_\sigma = 250$ for sequential loading with some tension release immediately prior to failure; and

$K_\sigma = 400$ is usually chosen for structural elements. This softening is less severe than that proposed by Vecchio and Collins (1986). This may be attributed to the orientation of the reinforcements: 45 deg to the principal directions for Vecchio and Collins, and parallel to the principal directions for Belarbi and Hsu (1995). The amount of reinforcement, especially transverse, is therefore also different between Vecchio and Collins and Belarbi and Hsu.

Tanabe and Wu (1991) presented some Japanese experimental results for biaxial tension-compression and the corresponding softening coefficient. Okamura and Maekawa (1987) proposed the following softening coefficient based on measurements of reinforced cylindrical specimens under axial compression and internal pressure

$$\beta = 1.0 \text{ for } \epsilon_1 < \epsilon_a \quad (30)$$

$$\beta = 1.0 - 0.4 \frac{\epsilon_1 - \epsilon_a}{\epsilon_b - \epsilon_a} \text{ for } \epsilon_a \leq \epsilon_1 \leq \epsilon_b$$

$$\beta = 0.6 \text{ for } \epsilon_b < \epsilon_1$$

where $\epsilon_a = 0.0012$ and $\epsilon_b = 0.0044$. Eq. (30) is identical to Eq. (20).

Shirai (1989) performed tests of small reinforced panels and proposed

$$\beta_1 = - \left(\frac{0.31}{\pi} \right) \tan^{-1} (4820 \epsilon_1 - 11.82) + 0.84 \quad (31)$$

$$\beta_2 = -5.9 - \frac{\sigma_1}{f'_c} + 1.0$$

$$\beta = \beta_1 * \beta_2$$

Some researchers have opted for a constant softening factor. Kupfer, Mang, and Karavesyrogliou (1983) used an experimental softening factor of 0.85 coupled with a sustained load factor of 0.80

$$f_{c2} = 0.80 \times 0.85 \times f'_c \approx \frac{2}{3} f'_c \quad (32)$$

Kupfer and Bulicek (1991) used

$$f_{c2} = f'_c \times 0.85 \times 0.75 \left(1 - \frac{f'_c}{250 \text{ MPa}} \right) \quad (33)$$

where

0.85 = factor for sustained load;
0.75 = factor for irregular crack trajectory; and
 $1 - f'_c / (250 \text{ MPa})$ = difference between cylinder strength and uncracked concrete prism.

For Reineck (1982, 1991), the strength of the web struts is not lower than

$$f_{cw} = 0.80 f'_c \quad (34)$$

In a recent paper on beam shear strength, Prisco and Gambarova (1995) used Hsu's (1993) formulation. To account for the effects of transverse reinforcement in tension, the concrete strength is reduced in one of two possible ways

$$f_c = 0.75 f'_c \text{ or } f_c = \frac{0.90 f'_c}{\sqrt{1 + 600 \epsilon_1}} \geq \frac{f'_c}{2} \quad (35)$$

The various formulas for biaxial softening are plotted in Fig. 9(a) and (b) for $\epsilon_1 / \epsilon_2 = -5$, a typical ratio for a beam in shear, and $f'_c = 35 \text{ MPa}$. It can be seen that a consensus has yet to be reached among researchers on whether the concrete softening

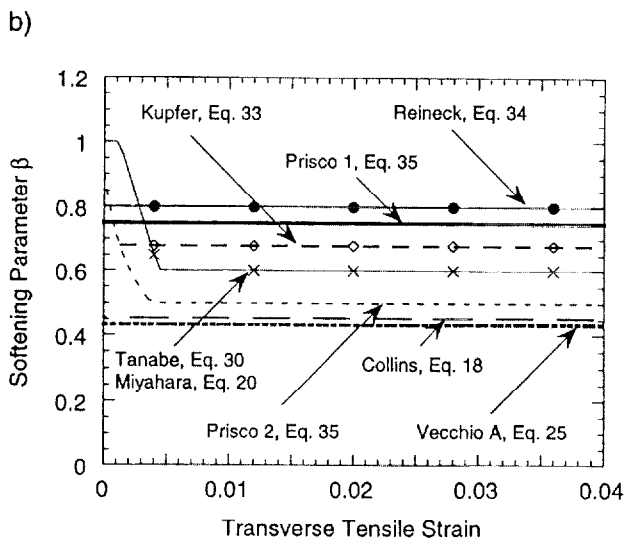
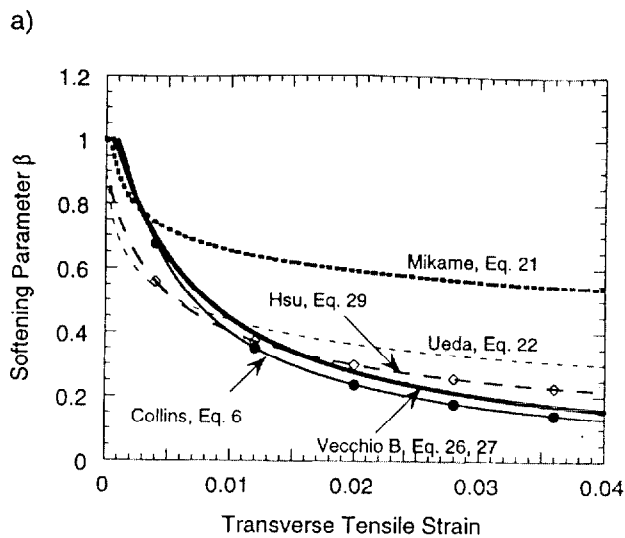


Fig. 9—Softening parameter for $\epsilon_1/\epsilon_2 = -5$ and $f'_c = 35$ MPa according to various researchers.

parameter is constant, or dependent on the average principal tensile stress or strain. The question this paper addresses is: how do these various formulations affect beam shear strength? The tool used for this purpose is the MCFT.

PARAMETRIC STUDY

As mentioned in the previous review, the MCFT accounts for shear transfer across cracks and concrete softening due to the biaxial state of tension-compression in the web of beams loaded in shear. Since many different formulations for shear friction and concrete softening exist, a parametric study is performed using the MCFT to determine the influence of these two factors on beam shear strength. For this purpose, the computer program SHEAR and two example beams (Fig. 10) are adapted from Collins and Mitchell (1991). SHEAR can predict the load-deformation response of reinforced or prestressed concrete beams subjected to shear or shear combined with axial load. At each step, the user inputs a value of principal tensile strain ϵ_1 , and the program assumes a strut angle θ , then computes strains, loads, crack widths, etc. according to a 17-step procedure used by Collins and Mitchell (1991) to implement the MCFT. In particular, Eq. (3), (4), and (6) are coded into SHEAR. If convergence is not achieved, another value of θ is tried. The program stops when equilibrium cannot be achieved

Table 1—Measured and predicted shear strength of prestressed concrete (PC) Beam CF1

Test	465 kN
AASHTO	400 kN
SHEAR	414 kN
RESPONSE	439 kN
DUALSECTION	469 kN
ACI	443 kN, 498 kN

Table 2—Stirrup and crack spacing for PC beam

Stirrup bar no.	s , mm	ρ_v , percent	s_{max} , mm	s_{min} , mm
2 (smooth)	355	0.12	414	1252
2 (smooth)	152	0.28	414	602
3	152	0.61	414	295
4	152	1.11	414	246

after a specified number of iterations, due to concrete crushing or all reinforcement yielding.

The base case ($F = \tau/\tau_{max} = 0.18$, $\rho_v = 0.61$ percent) corresponds to a PC beam tested by Arbesman and Conte (1973) [Fig. 10(a) and (b)] and used as an example by Collins and Mitchell. The measured strength of the beam was 465 kN versus a prediction of 414 kN by SHEAR. The calculation was performed at the critical section, a distance d_v away from the face of the support. At that location, the moment-to-shear ratio is 254 mm, and this moment is accounted for in SHEAR by an equivalent axial tension $2M/d_v$. The results show that, of the four methods based on the MCFT, the simple hand method given in AASHTO produces the most conservative result (predicted capacity equals 86 percent of observed capacity), and the three computer-based solutions—SHEAR, RESPONSE, and DUALSECTION—give progressively more accurate predictions as the analysis becomes more complex. On the other hand, the ACI sum of web-shear cracking and stirrup capacity for a section at a distance $h/2$ of half the section depth from the support face gives $V_{cw} + V_s = 325$ kN + 173 kN = 498 kN. At the support face of the test span—moments are highest at the support and at load $2P$ —the ACI equations predict a shear capacity of $V_{ci} + V_s = 270$ kN + 173 kN = 443 kN (Table 1).

Shear friction

As mentioned previously, shear friction enters into the MCFT as a parameter $F = \tau/\tau_{max} = 0.18$, with τ_{max} a function of crack width w and maximum aggregate size c [Eq. (2b) and (3)]. This shear friction parameter was varied between arbitrary values of $0.35 \times 0.18 = 0.063$ and $1.5 \times 0.18 = 0.27$. Computer program SHEAR was modified by varying F .

Shear friction of prestressed concrete beams

Fig. 11(a), (b), and (c) show the computed shear force V versus crack width w relationship for a concrete strength of $f'_c = 38.6$ MPa, various combinations of shear friction parameter ($F = 0.063, 0.18, \text{ or } 0.27$), and area of shear reinforcement ($\rho_v = 0.12, 0.28, 0.61, \text{ or } 1.11$ percent). The shear reinforcement uses No. 2 bars (smooth, $\phi = 6$ mm) at 355- or 152-mm spacing, No. 3 or No. 4 bars (deformed, $\phi = 9.5$ or 13 mm) at 152-mm spacing. As the shear reinforcement varies, so does its crack control characteristics (s_{max}, s_{min}) that must be input into the program (Table 2). The shear reinforcement obeys ACI design guidelines.

Maximum shear reinforcement ratio (ACI Section 11.5.6.8)

$$\rho_v = \frac{A_v}{b_w s} \leq \frac{8 \sqrt{f'_c} / \text{psi}}{f_y / \text{psi}}$$

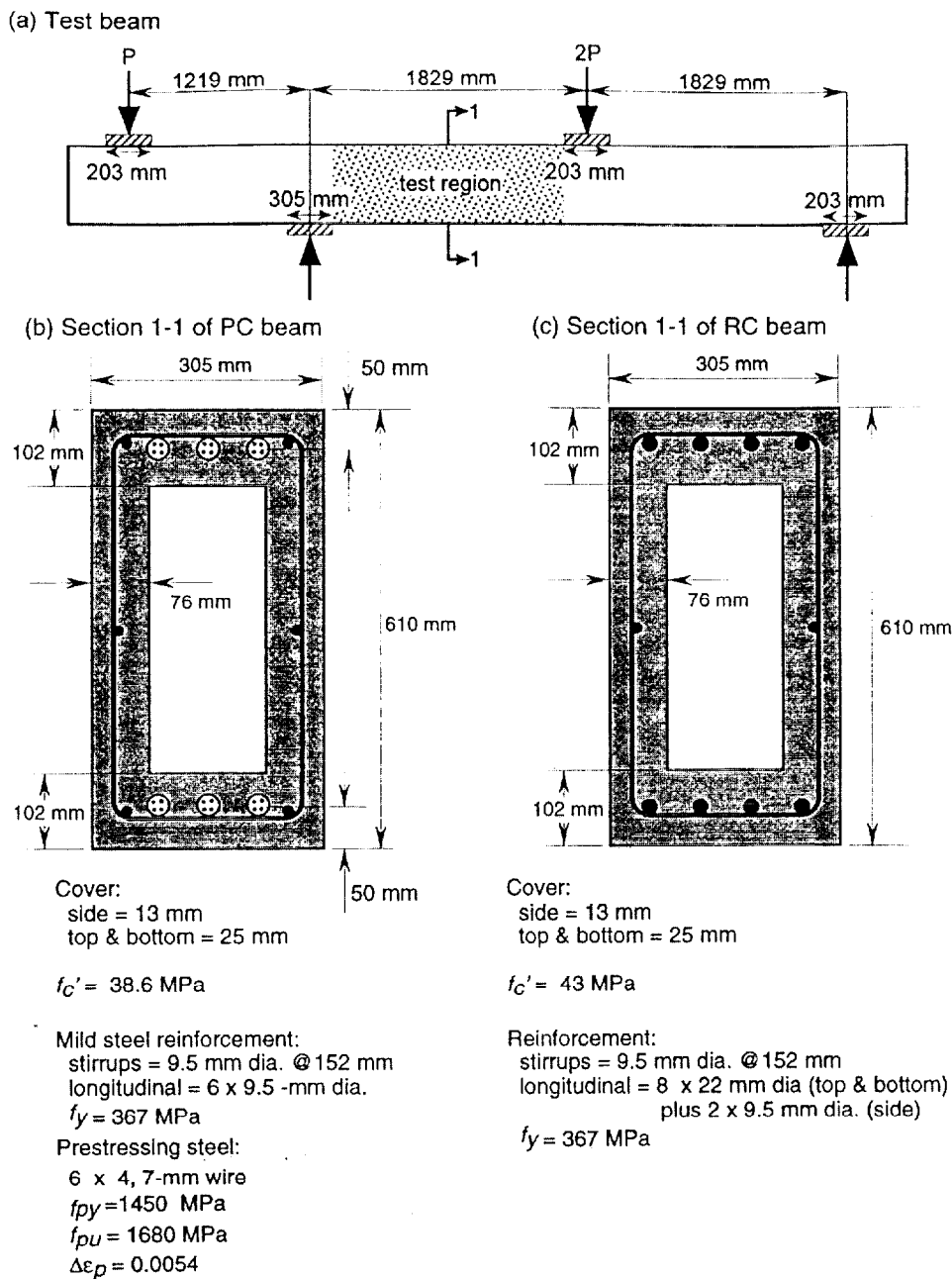


Fig. 10—Configuration of beams used in parametric study: (a) load configuration; (b) prestressed Beam CF1; and (c) reinforced concrete beam (adapted from Collins and Mitchell, 1991).

$$\text{or } \rho_v = \frac{A_v}{b_w s} \leq \frac{0.7 \sqrt{f'_c} / \text{MPa}}{f_y / \text{MPa}} = \frac{0.7 \sqrt{38.6}}{367} = 1.2 \text{ percent}$$

$$s \leq 0.75h = 0.75 \times 610 \text{ mm} = 457 \text{ mm}$$

Maximum stirrup spacing (ACI Section 11.5.5.4)

$$s \leq \frac{A_v f_y}{f_{pu} A_{ps}} \frac{80}{d} \sqrt{\frac{b_w}{d}}$$

$$s \leq \frac{64.5 \text{ mm}^2 \times 367 \text{ MPa}}{1682 \text{ MPa}} \frac{80}{926 \text{ mm}^2} 559 \text{ mm} \sqrt{\frac{152 \text{ mm}}{559 \text{ mm}}}$$

$$= 355 \text{ mm}$$

or (ACI Section 11.5.4.1)

Minimum shear reinforcement

$$\rho_v \geq \frac{50 \text{ psi}}{f_y}$$

$$\text{or } \rho_v \geq \frac{0.345 \text{ MPa}}{f_y} = \frac{0.345}{367} = 0.094 \text{ percent}$$

For this comparison, SHEAR was run for a section with zero moment (midspan). In all cases, failure was by diagonal compression (concrete crushes, symbol *c* in curves), preceded by stirrup yielding (symbol *y*) and crack slipping (symbol *s*). The program was run until failure, even after crack widths had

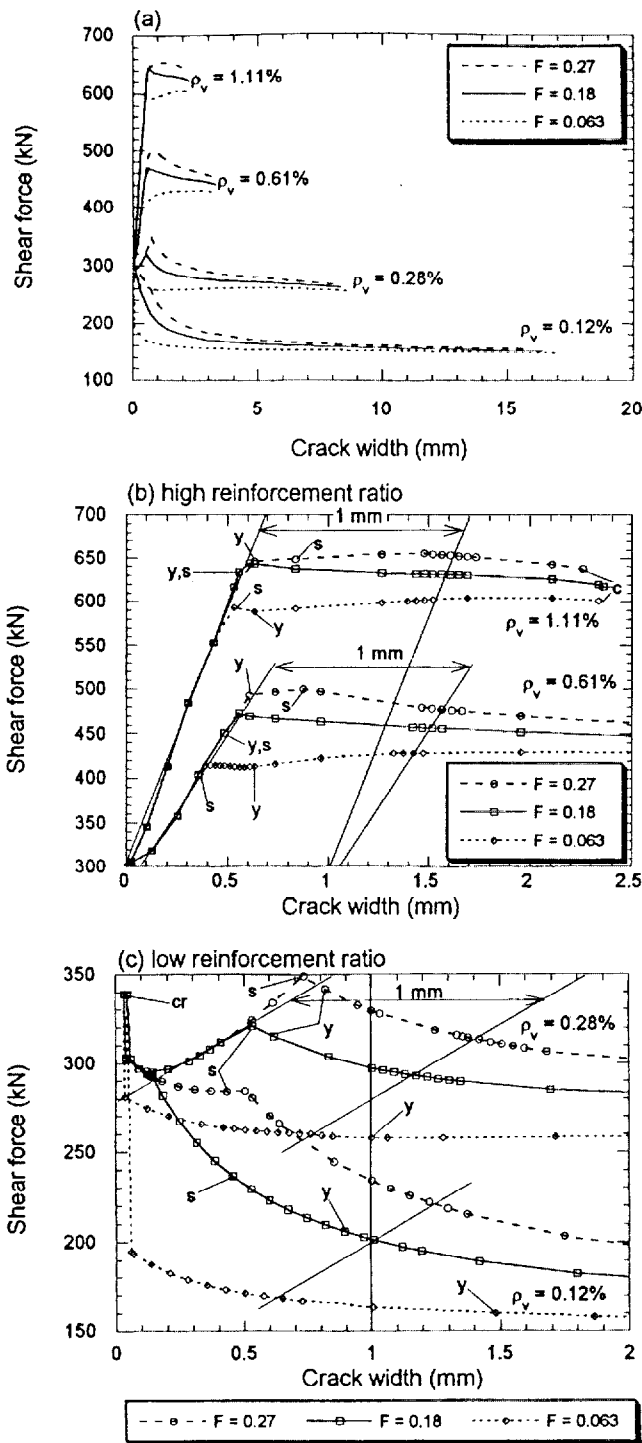


Fig. 11—Effect of shear friction and shear reinforcement on prestressed concrete behavior (cr = initial cracking; y = stirrup yield; s = crack slip; c = concrete crushes). (Note: $f'_c = 38.6$ MPa.)

reached unrealistic values (the range of shear friction laws only extends to $w \leq 1.5$ mm) to show the increase in ductility as the amount of shear reinforcement or the shear friction parameter decreases. Also, as crack widths increase, the $V-w$ curves for various friction parameters approach one another as they should, since shear friction approaches zero. Two types of behavior can be observed.

For high and medium shear reinforcement ratio [$\rho_v > 0.3$ percent, Fig. 11(b)], the curve $V-w$ typically follows a linear path up to stirrup yielding or crack slipping. The latter occurs when tension in the concrete reaches a limit imposed by the shear reinforcement and shear friction across cracks

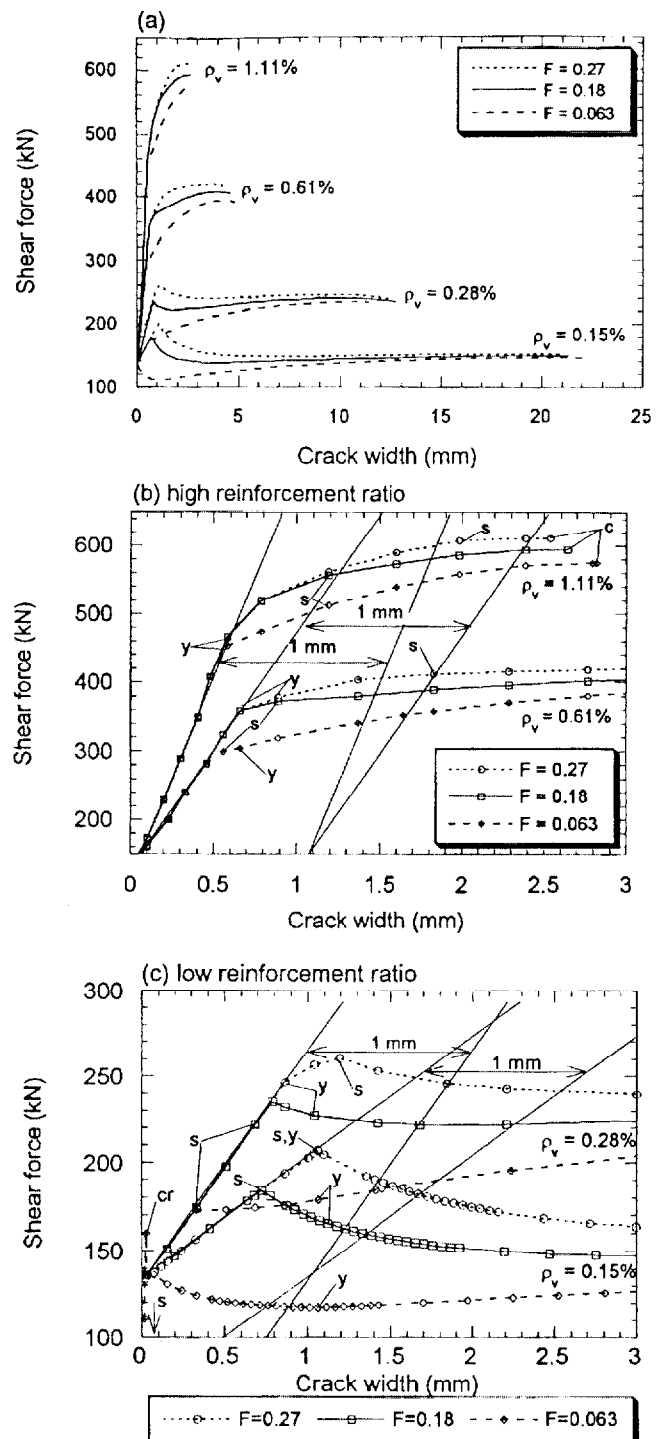


Fig. 12—Effect of shear friction and shear reinforcement on reinforced concrete behavior (cr = initial cracking; y = stirrup yield; s = crack slip; c = concrete crushes). (Note: $f'_c = 43$ MPa.)

$$f_{Vlimit} = v_{ci} \tan \theta + \frac{A_v}{b_w s} (f_{vy} - f_v)$$

For high friction, stirrups yield before cracks slip; for low friction, the order is reversed; and for medium friction, stirrup yielding and crack slipping occur simultaneously. Peaks of shear force V occur at initiation of crack slipping, although for low friction it's only a local peak (V in this case reaches its global peak at large crack widths $w > 2$ mm).

For low shear reinforcement, the shear force reaches a peak at a small crack width ($w < 0.05$ mm), then drops precipitously

Table 3—Variation of shear force V of PC beam for various values of shear friction F and stirrup ratio ρ_v

F	0.27			0.18			0.63			Method
	θ deg	V_i kN	Percent	θ deg	V_i kN	Percent	θ deg	V_i kN	Percent	
1.11	29.3	653.1	103	29.5*	632.7*	100	28.6*	602.2*	95	1 mm offset
	30.9	646.7	100	30.9*	645.0*	100	29.9*	593.4*	92	Linear limit
	29.5	655.7	102	30.9*	645.0*	100	28.3*	604.5*	94	Peak
0.61	24.3	477.3	105	23.9	456.5	100	23.2	428.3	94	1 mm offset
	26.8	492.8	104	26.5	472.8	100	25.6	414.1	88	Linear limit
	25.8	500.5	106	26.5	472.8	100	22.7	429.7	91	Peak
0.28	20.8	318.7	107	20.5	297.3	100	19.9	261.8	88	1 mm offset
	21.6	329.6	111	20.5	297.3	100	19.0	258.0	87	$w = 1$ mm
	22.6	348.9	109	22.2	321.0	100	22.4	281.1	86	Peak
0.12	17.2	222.2	110	16.4	201.5	100	14.9	169.3	84	1 mm offset
	18.0	234.3	116	16.4	201.5	100	14.2	163.6	81	$w = 1$ mm
	21.5	284.3	97	22.6	292.1	100	17.1	194.7	67	Slope

*Results obtained using Eq. (2) or (3).

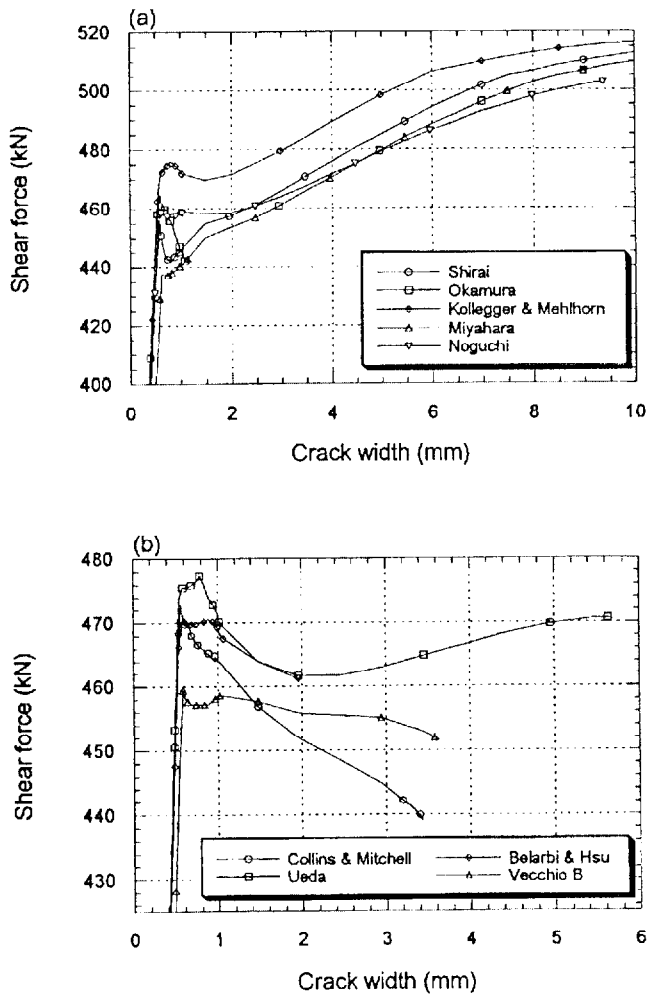


Fig. 13—Effect of concrete biaxial softening on shear behavior of prestressed concrete beam.

when concrete starts to crack. For $\rho_v = 0.28$ percent, after the initial drop, the load recovers and increases to a maximum until cracks start to slip, at which point it starts to decrease [Fig. 11 (c)]. For $\rho_v = 0.28$ percent and low friction, and for $\rho_v = 0.12$ percent, there is no load increase after the initial sharp drop at initial cracking. However, for $\rho_v = 0.12$ percent and high or medium friction, a change of slope is still noticeable at initial crack slip.

Table 4—Stirrup and crack spacing for reinforced concrete (RC) beam

Stirrup bar no.	s , mm	ρ_{cv} , percent	s_{mL} , mm	s_{mE} , mm
2 (smooth)	280	0.15	340	1008
2 (smooth)	152	0.28	340	602
3	152	0.61	336	302
4	152	1.11	333	251

Because the shapes of the V - w curves vary [Fig. 11(b) and (c)], several methods are used to compare them:

- Peaks of V are used. For $\rho_v = 0.12$ percent, peaks degenerate to points of sudden change in negative slope.
- Values of V at $w = 1$ mm are selected.
- Where a linear part exists (prior to crack slipping or stirrup yielding), the values of V at the end of the linear range are selected.
- Intersections of the curves with a straight line parallel but offset with respect to the linear part by $w = 1$ mm are also used.
- Finally, where a linear part does not exist (e.g., for $\rho_v = 0.12$ percent), intersections of the curves with a straight line passing through the value of V at $w = 1$ mm for medium friction and parallel to the initial slope of the closest set of curves with a definable initial slope (here, $\rho_v = 0.28$ percent) are used.

Results are shown in Table 3.

Shear friction of reinforced concrete beams

Fig. 10(c) shows the RC beam used in this study. The RC beam has the same external dimensions as the PC beam, but the longitudinal reinforcement now consists of eight No. 7 bars ($\phi = 22$ mm) top and bottom and two No. 3 bars ($\phi = 9.5$ mm) at mid-depth for crack control. The concrete cylinder strength is 43 MPa, and the shear reinforcement, similar to that of the PC beam, also satisfies ACI requirements ($.094$ percent $\leq \rho_v \leq 1.2$ percent). Stirrup spacing does not exceed $d/2 = 280$ mm. Stirrups consist of No. 4 bars ($\phi = 13$ mm), No. 3 bars ($\phi = 9.5$ mm) or No. 2 smooth bars ($\phi = 6$ mm) at 152 mm. An additional configuration is No. 2 bars at 280 mm. These correspond to shear reinforcement ratio of $\rho_v = 1.11, 0.61, 0.28,$ and 0.15 percent, respectively (Table 4). Behavior is similar to that of the PC beam previously described. All beams failed by concrete crushing; the longitudinal reinforcement did not yield. Quantitative comparison is easier in this case than for the PC beam, because in all cases, an initial straight line can be defined, and the 1-mm offset method is straightforward (Table 5 and Fig. 12).

Table 5—Variation of shear force V of RC beam for various values of shear friction F and stirrup ratio ρ_v

F	0.27			0.18			0.63			Method
	ρ_v percent	θ deg	V_i kN	Percent	θ deg	V_i kN	Percent	θ deg	V_i kN	
1.11	31.4	600.4	104	31.3	579.7	100	31.0	546.0	94	1-mm offset
0.61	28.1	412.3	106	28.0	387.2	100	27.7	352.2	91	1-mm offset
0.28	26.3	245.8	111	24.7	221.8	100	26.3	184.3	83	1-mm offset
0.15	24.7	174.6	114	24.9	159.8	100	25.4	118.2	77	1-mm offset
0.28	29.6	260.8	111	20.1	235.3	100	35.0	172.4	73	Peak or linear limit
0.15	29.7	206.9	112	31.2	184.0	100	44.0	135.9	74	Peak or linear limit

Table 6—PC beam: shear force for various biaxial softening laws*

Model	V_L , kN	V_L/V_N , percent	w_L , mm
Kollegger	476	111	0.8
Shirai	455	106	0.6
Okamura	465	108	0.6
Miyahara	438	102	0.6
Noguchi	460	107	0.6
Ueda	477	111	0.8
Hsu	471	110	0.6
Vecchio-B	459	107	0.6
Collins	473	110	0.7

* $\rho_v = 0.61$ percent. Subscript L for end of linear range. V_N = experimental shear strength.

For both PC and RC beams, the following is observed:

- As the shear reinforcement ratio decreases, the effect of shear friction increases. This is to be expected since, as shear reinforcement decreases, the proportion of shear load carried by shear friction increases. For a shear friction parameter of 35 percent of the base case, as in HSC compared to NSC, the shear force V at or near its peak is 15 to 25 percent lower than for the base case, depending on the method of estimation.
- Two cases were run for the PC beam (for $f'_c = 38.6$ MPa, $\rho_v = 1.11$ percent, $F = 0.18$ or 0.063) using the 1986 version of the MCFT, which has a more elaborate shear friction law [Eq. (2)] compared with the 1991 version [Eq. (3)]. The results of the two versions are indistinguishable from each other, i.e., the normal compressive stress σ across shear cracks is negligible.
- Failure by concrete crushing is predicted to occur at high w (very wide cracks), much higher than the range of Walraven's experimental data ($v \leq 2$ mm, $w \leq 1.5$ mm).

Biaxial softening

Computer program SHEAR was modified by replacing Eq. (4) and (6) with various biaxial softening models and was run for a zero moment section. For the PC beam (Fig. 13), in cases where SHEAR did not predict concrete crushing, the program was stopped after large crack widths were attained (approximately 20 mm). The curve shear force versus crack width ceases to be linear shortly after stirrups yield and cracks slip. Peaks (local peaks, in some cases) occur near that point and are compared in Table 6. Two types of behavior are observed for the various softening models (Fig. 13 and Table 6).

- Significant postlinear strength gain is predicted by the models of Kollegger, Okamura, Miyahara, and Shirai that predict no concrete crushing (failure is by excessive deformation); and the models of Ueda and Noguchi, which predict fairly similar behavior, concrete crushing

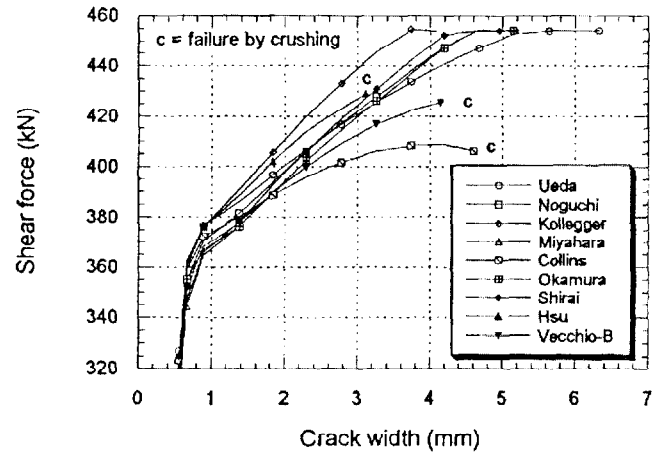


Fig. 14—Effect of concrete biaxial softening on shear behavior of reinforced concrete beam.

after considerable postlinear strength, and wide cracks.

- No postlinear strength gain is predicted by the models of Collins, Vecchio-B [Eq. (26)], and Hsu.
- For the RC beam, the various models start deviating from linearity (of the $V-w$ curve) and from each other when stirrups yield, followed shortly afterwards by crack slipping. Two types of behavior are predicted:
- Diagonal compression failure (concrete crushing) is predicted by the models of Collins, Vecchio-B [Eq. (26)], and Hsu.
 - Shear tension failure (yielding of the longitudinal reinforcement) is predicted by the models of Ueda, Noguchi, Kollegger, Miyahara, Okamura, and Shirai. Ueda's model comes close to predicting a balanced failure by both compression and tension. Results are shown in Fig. 14 and Table 7.

CONCLUSION

Laws for shear friction and biaxial softening of concrete used in various beam shear theories vary widely. The modified compression field theory (MCFT) was used to study the effects of various shear friction and concrete softening formulations on the calculated shear strength of PC and RC beams. According to the MCFT, a decrease in shear friction within the range of experimental data, as found, for example, in high-strength concrete, lowers the shear strength of beams with low shear reinforcement by 15 to 25 percent, depending on the method of estimation.

In addition, a comparison was presented of different relationships used to represent the biaxial compression-tension strength of reinforced concrete. For PC beams where the prestressing cables do not fail, some theories of biaxial softening of concrete do not predict concrete crushing, even for very high

Table 7—RC beam: shear force for various biaxial softening laws*

Model	V_{max} , kN	V_{max} percent of smallest	w_{max} , mm	At last iteration (1000 $\epsilon_y = 1.83$)			Mode of failure
				f_s , MPa	$f_{s,max}$, MPa	1000 ϵ_r	
Ueda	454	111	6.3	17.4	19.8	1.81	Tension
Noguchi	454	111	5.2	17.2	25.3	1.78	Tension
Kollegger	454	111	4.1	17.1	43.0	1.77	Tension
Miyahara	437	107	3.7	17.3	25.8	1.80	Tension
Okamura	454	111	5.2	17.3	25.8	1.80	Tension
Shirai	454	111	5.0	17.4	29.3	1.80	Tension
Collins	409	100	4.6	13.7	14.1	1.35	Compression
Hsu	429	105	3.1	14.8	15.3	1.47	Compression
Vecchio-B	426	104	4.1	14.8	17.2	1.48	Compression

* $\rho_v = 1.11$ percent.

deformations. For RC beams, some models predict shear tension failure, while others predict diagonal compression failure. However, the peak shear forces that occur close to stirrup yielding and crack slipping are within 10 percent of each other for the various theories and of the test value for the PC beam.

ACKNOWLEDGMENTS

Michael P. Collins, Julio A. Ramirez, and Nicholas J. Carino reviewed early drafts of this paper and offered valuable suggestions. Wilasa Vichit-Vadakan helped with some of the computer runs and graphics. To all, the author extends his thanks.

NOTATIONS

- A_v = area of shear reinforcement
- a_x, a_y = projection parallel, perpendicular to crack of contact area between aggregate and mortar
- b_w = beam width
- c = maximum size of aggregate
- d = beam depth, from extreme compression fiber to centroid of tension reinforcement
- d_v = distance measured perpendicular to neutral axis between resultants of tensile and compressive forces due to flexure, but need not be taken less than $0.9d$
- F = friction parameter
- f'_c = concrete cylinder strength or uniaxial compressive strength
- f'_{ce} = concrete cube strength or uniaxial compressive strength
- f'_{c1} = principal tensile stress in concrete web
- f'_{c2} = principal compressive stress in concrete web
- $f'_{c2,max}$ = compressive strength of concrete panel in biaxial tension-compression
- $f'_{c2,base}$ = uniaxial compressive stress for Thorenfeldt curve
- f'_{cw} = compressive strength of concrete web
- f'_p = maximum compressive stress for softened concrete
- f_t = concrete tensile strength
- f_v = stress in shear reinforcement
- f_{yv}, f_y = yield strength of shear reinforcement
- jd = beam shear depth
- h = overall section depth
- s = stirrup spacing
- s_{mv} = crack control characteristics of transverse reinforcement
- s_{mr} = crack control characteristics of longitudinal reinforcement
- V = shear force, shear strength
- V_c = concrete contribution to shear strength
- V_{c1} = shear force at flexure-shear cracking
- V_{c2} = shear force at web-shear cracking
- V_s = steel contribution to shear strength
- V_x = experimental shear strength
- v = crack slip
- v_{t1}, τ = shear stress at crack interface
- w = crack opening
- β = softening parameter
- ϵ_0 = strain at maximum compressive stress for uniaxial compression
- ϵ_1 = principal tensile strain in concrete
- ϵ_2 = principal compressive strain in concrete
- ϵ_{1L} = concrete tensile strain at which reinforcement at crack begins to yield
- ϵ_p = strain corresponding to f_p
- ϵ_y = yield strain of shear reinforcement

- θ = strut angle
- μ = friction coefficient between aggregate and mortar
- ρ_v = shear reinforcement geometrical ratio
- σ = normal stress across a crack
- σ_{pv} = mortar strength
- τ_0 = cohesion friction stress (for $\sigma = 0$)
- τ_{max} = maximum shear stress transmitted across crack
- ϕ = crack angle, bar diameter
- ω = shear reinforcement mechanical ratio

REFERENCES

AASHTO (American Association of State Highway and Transportation Officials), 1992. *LRFD Bridge Design Specifications*, 1st edition, Washington, D.C., 1091 pp.

ACI Committee 318, 1995. "Building Code Requirements for Reinforced Concrete (318-95) and Commentary (318-95R)," American Concrete Institute, Farmington Hills, Mich., 369 pp.

Arbesma, B., and Conte, D. F., 1973. "The Design and Testing to Failure of a Prestressed Concrete Beam Loaded in Flexure and Shear," BASc thesis, University of Toronto, 176 pp.

Bazant, Z., and Gambarova, P., 1980. "Rough Cracks in Reinforced Concrete," *ASCE*, V. 106, No. ST4, Apr., pp. 819-841.

Belarbi, A., and Hsu, T. C., 1991. "Constitutive Laws of RC in Biaxial Tension-Compression," *Research Report UHCEE 91-2*, University of Houston, Tex.

Belarbi, A., and Hsu, T. C., 1995. "Softened Concrete in Biaxial Tension-Compression," *ACI Structural Journal*, V. 92, No. 5, Sept.-Oct., pp. 562-573.

Bhude, S. B., and Collins, M. P., 1989. "Influence of Axial Tension on Shear Capacity of Reinforced Concrete Members," Sept.-Oct., pp. 570-581.

Collins, M. P., and Mitchell, D., 1991. *Prestressed Concrete Structures*, Prentice-Hall, Inc., Englewood Cliffs, N. J., 766 pp.

Collins, M. P., and Porasz, A., 1989. "Shear Design for High-Strength Concrete," *CEB Bulletin d'Information* No. 193—Design Aspects of Concrete, pp. 75-83.

CSA (Canadian Standards Association), 1994. *Design of Concrete Structures*, CSA A23.3-94, Dec., 200 pp.

Dei Poli, S.; Prisco, M. D.; and Gambarova, P. G., 1990. "Stress Fields in Web of Reinforced Concrete Thin-Webbed Beams Failing in Shear," *Journal of Structural Engineering*, V. 116, No. 9, Sept., pp. 2496-2515.

Fréney, J. W., 1990. "Theory and Experiments on Behavior of Cracks in Concrete Subjected to Sustained Shear Loading," *Heron*, V. 35, No. 1, Delft University of Technology, 80 pp.

Fréney, J. W., 1985. "Shear Transfer across Single Crack in Reinforced Concrete under Sustained Loading: Part I—Experiments," *Stevin Report* 5-85-5, 114 pp.

Fréney, J. W.; Pruijssers, A. F.; Reinhardt, H. W.; and Walraven, J. C., 1987. "Shear Transfer in High-Strength Concrete," *Proceedings, Symposium on Utilization of High-Strength Concrete*, Stavanger, Norway, June, pp. 225-235.

Hofbeck, J. A.; Ibrahim, I. O.; and Mattock, A. H., 1969. "Shear Transfer in Reinforced Concrete," *ACI JOURNAL*, *Proceedings* V. 66, No. 2, Feb., pp. 119-128.

Hognestad, E., 1952. "What Do We Know about Diagonal Tension and Web Reinforcement in Concrete?" *Circular Series*, No. 64, University of Illinois Engineering Exp. Station, Ill., 47 pp.

Hsu, T., 1993. *Unified Theory of Reinforced Concrete*, CRC Press, 313 pp.

Joint ASCE-ACI Task Committee 426, 1973. "The Shear Strength of Reinforced Concrete Members," *Journal of the Structural Division*, ASCE ST6.

- Kollegger, J., and Mehlhorn, G., 1987. "Material Model for Cracked Reinforced Concrete," IABSE Colloquium on Computational Mechanics of Concrete Structures: Advances and Applications, Delft, *Report No. 54*, pp. 63-74.
- Kollegger, J., and Mehlhorn, G., 1990. "Material Model for Analysis of Reinforced Concrete Surface Structures," *Computational Mechanics*, Springer Verlag, No. 6, pp. 341-357.
- Kupfer, H., and Bulicek, H., 1992. "A Consistent Model for Design of Shear Reinforcement in Slender Beams with I- or Box-Shaped Cross Section," *Proceedings, Symposium on Concrete Shear in Earthquake*, Houston, Tex., pp. 256-265.
- Kupfer, H.; Mang, R.; and Karavesyroglou, M., 1983. "Ultimate Limit State of Shear Zone of Reinforced and Prestressed Concrete Girders—An Analysis Taking Aggregate Interlock into Account," *Bauingenieur* 58, pp. 143-149. (in German)
- MacGregor, J. G., 1992. *Reinforced Concrete: Mechanics and Design*, 2nd edition, Prentice Hall, Englewood Cliffs, N. J., 848 pp.
- Mau, S. T., and Hsu, T. T., 1988. Discussion of paper by Walraven, J. C., Fréney, J., and Pruijssers, A., "Influence of Concrete Strength and Load History on Shear Friction Capacity of Concrete Members," *PCI Journal*, V. 22, No. 1, Jan.-Feb. 1988, pp. 166-170.
- Mikame, A.; Uchida, K.; and Noguchi, H., 1991. "A Study of Compressive Deterioration of Cracked Concrete," *Proceedings, International Workshop on FEA of RC*, Columbia University, New York.
- Miyahara, T.; Kawakami, T.; and Maekawa, K., 1988. "Nonlinear Behavior of Cracked Reinforced Concrete Plate Element under Uniaxial Compression," *Proceedings, Japan Society of Civil Engineers*, V. 11, pp. 306-319. Also in *Concrete Library International*, JSCE, No. 11, June, pp. 131-144.
- Norwegian Council for Building Standardization, 1992. *Norwegian Standard NS 3473 E*, 4th edition, Nov.
- Okamura, H., and Maekawa, K., 1987. "Nonlinear Analysis of Reinforced Concrete," *Proceedings of JSCE*, No. 360, Aug., pp. 1-10.
- Paulay, T., and Loeber, P. J., 1974. "Shear Transfer by Aggregate Interlock," *Shear in Reinforced Concrete*, SP-42, American Concrete Institute, Farmington Hills, Mich., pp. 1-15.
- Prisco, M. D., and Gambarova, P. G., 1995. "Comprehensive Model for Study of Shear in Thin-Webbed RC and PC Beams," *Journal of Structural Engineering*, V. 121, No. 12, Dec., pp. 1822-1831.
- Prujssers, A. F., and Liqui Lung, G., 1985. "Shear Transfer across Crack in Concrete Subjected to Repeated Loading: Experimental Results—Part I," *Stevin Report*, 178 pp.
- Reineck, K. H., 1982. "Models for Design of Reinforced and Prestressed Concrete Members," *CEB Bulletin d'Information* No. 146—Shear in Prestressed Concrete, Jan.
- Reineck, K. H., 1991. "Modeling of Members with Transverse Reinforcement," IABSE Colloquium on Structural Concrete, Stuttgart, *IABSE Report*, V. 62, pp. 481-488.
- Shirai, S., and Noguchi, H., 1989. "Compressive Deterioration of Cracked Concrete," *Proceedings, Structures Congress—Design, Analysis and Testing*, ASCE, New York, pp. 1-10.
- Tanabe, T., and Wu, Z., 1991. "Strain Softening under Biaxial Tension and Compression," IABSE Colloquium on Structural Concrete, Stuttgart, *IABSE Report*, V. 62, pp. 623-636.
- Thorenfeldt, E.; Tomaszewicz, A.; and Jensen, J. J., 1987. "Mechanical Properties of HSC and Application in Design," *Proceedings, Symposium on Utilization of High-Strength Concrete*, Stavanger, Norway, June, pp. 149-159.
- Ueda, M.; Noguchi, H.; Shirai, N.; and Morita, S., 1991. "Introduction to Activity of New Reinforced Concrete," *Proceedings, International Workshop on FEA of Reinforced Concrete*, Columbia University, New York.
- Vecchio, F. J., and Collins, M. P., 1982. "The Response of Reinforced Concrete to In-Place Shear and Normal Stresses," *Publication 82.03*, University of Toronto, Mar., 332 pp.
- Vecchio, F. J., and Collins, M. P., 1986. "The Modified Compression Field Theory for Reinforced Concrete Elements Subjected to Shear," *ACI JOURNAL*, *Proceedings* V. 83, No. 2, Mar.-Apr., pp. 219-231.
- Vecchio, F. J., and Collins, M. P., 1993. "Compression Response of Cracked Reinforced Concrete," *ASCE Journal of Structural Engineering*, V. 119, No. 12, Dec., pp. 3590-3610.
- Vecchio, F. J.; Collins, M. P.; and Aspiotis, J., 1994. "High-Strength Concrete Elements Subjected to Shear," *ACI Structural Journal*, V. 91, No. 4, July-Aug., pp. 423-433.
- Walraven, J. C., 1995. "Shear Friction in High-Strength Concrete," *Progress in Concrete Research*, Delft University of Technology, V. 4, pp. 57-65.
- Walraven, J. C., 1981. "Fundamental Analysis of Aggregate Interlock," *Journal of the Structural Division*, ASCE, V. 107, No. ST11, Nov., pp. 2245-2270.
- Walraven, J. C.; Fréney, J.; and Pruijssers, A., 1987. "Influence of Concrete Strength and Load History on Shear Friction Capacity of Concrete Members," *PCI Journal*, V. 32, No. 1, Jan.-Feb., pp. 66-85.
- Walraven, J. C., and Reinhardt, H. W., 1981. "Theory and Experiments on Mechanical Behavior of Cracks in Plain and Reinforced Concrete Subjected to Shear Loading," *Heron*, V. 26, No. 1A, 68 pp.
- Walraven, J., and Stroband, J., 1994. "Shear Friction in High-Strength Concrete," *High-Performance Concrete: Proceedings, ACI International Conference, Singapore*, SP-149, V. M. Malhotra, ed., American Concrete Institute, Farmington Hills, Mich., pp. 311-330.